

Is the Lightest Kaluza–Klein Particle a Viable Dark Matter Candidate?

Géraldine Servant ^{a,b} and Tim M.P. Tait ^a

^a *High Energy Physics Division, Argonne National Laboratory, Argonne, IL 60439.*

^b *Enrico Fermi Institute, University of Chicago, Chicago, IL 60637*

servant@theory.uchicago.edu, tait@hep.anl.gov

Abstract

In models with universal extra dimensions (*i.e.* in which all Standard Model fields, including fermions, propagate into compact extra dimensions) momentum conservation in the extra dimensions leads to the conservation of Kaluza–Klein (KK) number at each vertex. KK number is violated by loop effects because of the orbifold imposed to reproduce the chiral Standard Model with zero modes, however, a KK parity remains at any order in perturbation theory which leads to the existence of a stable lightest KK particle (LKP). In addition, the degeneracy in the KK spectrum is lifted by radiative corrections so that all other KK particles eventually decay into the LKP. We investigate cases where the Standard Model lives in five or six dimensions with compactification radius of TeV^{-1} size and the LKP is the first massive state in the KK tower of either the photon or the neutrino. We derive the relic density of the LKP under a variety of assumptions about the spectrum of first tier KK modes. We find that both the KK photon and the KK neutrino, with masses at the TeV scale, may have appropriate annihilation cross sections to account for the dark matter, $\Omega_M \sim 0.3$.

1 Introduction

One of the most exciting open questions on the interface between particle physics and cosmology is the nature of the dark matter. In fact, observations indicate that most of the matter in the universe is dark, and cosmological evidence has accumulated to provide independent confirmations that a large part of the Dark Matter (DM) is non-baryonic. Recent measurements of the Cosmic Microwave Background anisotropy combined with measurement of the Hubble parameter suggest a flat universe in which 30% of the energy density is due to non relativistic matter and only 4% is due to baryons, consistent with measurements from clusters and Big Bang Nucleosynthesis (see [1,2] for recent reviews). In this paper we will use the value derived by Turner from combining all the current data [2]:

$$\begin{aligned}\Omega_M &= 0.33 \pm 0.035, \\ h &= 0.69 \pm 0.06,\end{aligned}\tag{1}$$

in which Ω_M is the matter density of the universe expressed as a fraction of the critical density for a flat universe. h is the normalized expansion rate ($H_0 = 100 h \text{ km s}^{-1}\text{Mpc}^{-1}$).

Observational evidence for DM has been building but we still have no solid clue as to its identity. Various candidates have been suggested and the theory of structure formation provides indirect evidence about some of its properties, strongly hinting that it is weakly interacting and non-relativistic at late times. In other words, it is cold dark matter (CDM). The standard model (SM) of particle interactions, while describing remarkably well the results of collider experiments, does not contain a suitable dark matter candidate, and thus it is necessary to consider extensions. There are essentially two well motivated DM candidates in this context: WIMPs and axions. WIMPs (Weakly interacting massive particles) were in thermal equilibrium with the Standard Model particles in the early universe. With masses in the 10–1000 GeV range and weak scale cross sections ($\sigma \sim 10^{-9} \text{ GeV}^{-2}$) they would have fallen out of equilibrium such that their relic density today would correspond to $\Omega_{\text{WIMP}} \sim \mathcal{O}(1)$. Axions, originally postulated to address the strong CP problem, would not have been produced at thermal equilibrium (but through the decay of axionic strings or domain walls for instance). Their mass is constrained by astrophysical and cosmological arguments to lie in the range $m \sim 10^{-5}\text{--}10^{-2} \text{ eV}$.

The most extensively studied DM candidate is the LSP (Lightest Supersymmetric Particle), a stable particle in supersymmetric (SUSY) models with conserved R-parity, which, in most SUSY scenarios, is the *neutralino* and is a typical WIMP. A broad range of experiments around the world are underway for detecting WIMPs, both through direct WIMP–nuclear scattering experiments and through indirect searches such as detection of cosmic flux from dark matter annihilation in the galactic center. Current searches are already exploring the parameter space of SUSY WIMPs. Unfortunately, SUSY models lack predictability. They contain a huge number of free parameters and one has to make several assumptions to reduce this number, for example by assuming a model to describe how supersymmetry is broken and how the effects of the supersymmetry breaking are communicated to the superpartners of the SM fields. For example, predictions for the

cosmic flux from annihilation of the LSP in the center of the galaxy can vary over orders of magnitude when scanning SUSY parameter space.

While the LSP is very well theoretically motivated, since the identity of the DM particles remains unconfirmed we should examine alternative possibilities. On the other hand, the DM issue sets important constraints on model building in particle theory. For any extension of the Standard model predicting the existence of a stable particle, one should compute its cosmological relic density to check whether it naturally accounts for DM or if it leads to overclosure of the universe in which case the model, or at least the cosmological picture associated with it, has to be revised.

The issue when searching for a dark matter candidate is to find a *stable* particle. There are two options: 1) The particle essentially does not interact with the Standard Model particles, has a very small decay rate, and therefore is stable on cosmological scales. 2) The particle is coupled to the SM. In this case, there must be a symmetry to guarantee its stability. In the case of the LSP, there is R-parity to guarantee the stability. In this paper, we study a new DM candidate: the LKP (Lightest Kaluza–Klein Particle¹) which interacts with SM particles and is stable because of a Kaluza–Klein parity. The LKP arises in a generic class of models in which all fields propagate in extra dimensions. The next section is devoted to explain these models, and the particle physics context. The model has many attractive features, including the fact that a relatively small number of parameters are sufficient to describe the LKP. Essentially one: its mass, which at tree level is the inverse of the compactification radius. In Section 3 we review the standard relic density computation. Our major work has been to calculate annihilation (and coannihilation) cross sections for the LKP in two cases. In the first case, the LKP is a Kaluza–Klein photon (Section 4), while in the second, it is a Kaluza–Klein neutrino (Section 5). We also study the effect of coannihilation in Section 6. Finally, Section 7 summarizes our results and discusses open questions which stimulate further work on the subject. Technical details are presented in the appendices.

2 Universal Extra Dimensions

Universal extra dimensions (UED) postulate that all of the SM fields may propagate in one or more compact extra dimensions [5]. This is to be contrasted with both the brane world scenario [6] where the SM fields are constrained to live in three spatial dimensions while gravity can propagate in the bulk, and intermediate models [7] in which only gauge bosons and Higgs fields propagate in extra dimensions while fermions live at fixed points. However, there is significant phenomenological motivation to having fermions and gauge bosons living in the bulk, including motivation for three families from anomaly cancellation [8], attractive dynamical electroweak symmetry breaking (EWSB) [10–12], (supersymmetric) models in which the Higgs mass is a calculable quantity [13], preventing rapid proton decay from non-renormalizable operators [9,14], orbifold breaking

¹The first discussion on the relic density of stable Kaluza–Klein particles (referred to as “pyrgons”) was made by Kolb and Slansky [3]. It was later alluded to in [4].

of the parity in left-right symmetric models [15], and (through the mechanism of fermion localization) natural explanations for the observed fermion masses and mixings [14,16–19]. In this article we discover a new motivation for the UED scenario: to provide a viable dark matter candidate.

The new feature of the UED scenario compared to the brane world is that since there is no brane to violate translation invariance along the extra dimensions, momentum is conserved at tree level leading to degenerate KK mode masses at each level and conservation of KK number in the interactions of the four dimensional effective theory. This statement is broken at the loop level, where the fact that the extra dimensions are compact leads to (calculable) violations of the full Lorentz symmetry [21], and as a result shifts the masses of the KK modes away from their tree level values.

Further violations result by applying orbifold boundary conditions in order to remove unwanted fermionic degrees of freedom. These lead to loop contributions that are log divergent [22] in the effective theory, thus signalling that they cannot be computed but must instead be treated as inputs. They further correct the KK mode masses and break conservation of KK number to conservation of KK parity², provided the terms induced at both of the orbifold fixed points are equal. Whether this will be true or not depends on the details of the compactification dynamics and the UV completion of the theory, but the assumption is self-consistent in the sense that if it is true at one scale, the cut-off scale for instance, it remains true at any scales since radiative corrections induce equal terms on both boundaries. The resulting theory has interactions only between even numbers of the odd-number KK modes. This conservation of KK parity implies that the lightest first level KK mode (LKP) cannot decay into SM zero modes and will be stable, in analogy with the lightest super-partner in a supersymmetric theory which conserves R -parity. Thus, UED is the first extra dimensional scenario to predict a candidate particle for dark matter. A further consequence of KK parity, that KK modes must be pair-produced, leads to interesting collider phenomenology [5,23].

At tree level the KK particles of a given level are predicted to be degenerate with masses n/R where R is the size of the compact dimension and n is the mode number. However, at loop level there are both calculable and in calculable corrections [20,21]. We follow the perspective of Ref. [21] and treat the divergent corrections as perturbations on the $1/R$ masses of the KK modes. This assumption is self-consistent though not completely general, and could occur, for example, if for some reason the underlying theory causes them to vanish at the cut-off scale ($\Lambda \lesssim 50R^{-1}$). This prescription was employed in Ref. [21] and results in small (loop-suppressed) corrections to the KK mass spectrum induced by renormalization group evolution from Λ to $1/R$. However, we do not strictly wed ourselves to the particular choice of the divergent corrections made in [21], but instead allow ourselves the freedom to adjust these terms independently in the effective theory.

For the LKP to be a well-motivated dark matter candidate, it should be electrically neutral and non-baryonic. Thus, the most promising candidates in the UED picture are first level KK modes of the neutral gauge bosons (analogues of the KK modes of the

²KK parity can be seen as the combination of a translation by πR with a flip of sign of all odd states in the KK Fourier decomposition of the bulk fields.

photon and Z), and the KK neutrino, $\nu^{(1)}$. One could also consider the first KK mode of the graviton, though this case seems less promising because its very weak gravitational interactions would imply that it will annihilate much less efficiently and could easily overclose the universe. Since similar incalculable loop corrections render the graviton mass a separate input of the theory, we may simply consider that the graviton is heavier than the LKP, such that at the time scales of interest to us all of the KK gravitons have already decayed into the LKP and zero modes. Alternately, one could consider a “deconstructed model” [24] in which the extra dimension is represented by a chain of gauge groups and thus there need not be KK modes of the graviton. A simple two-site model can successfully reproduce the physics of the first level KK modes, and would be sufficient for our purposes. More convincingly, there is actually an argument for having the KK graviton heavier than the lightest KK neutral gauge boson. While the KK graviton receives negligible radiative corrections in contrast with the KK states of the SM particles and therefore has a mass equal to R^{-1} , one can easily see from Ref. [21] (see next paragraph) that the lightest state which diagonalizes the $(B^{(1)}, W_3^{(1)})$ mass matrix is lighter than R^{-1} for $R^{-1} \gtrsim 800$ GeV. This is because $B^{(1)}$ receives negative radiative corrections. So even in the absence of boundary terms, the LKP, while being nearly degenerate with the KK graviton (the mass difference is less than 0.1 %) is indeed the KK photon for $R^{-1} \gtrsim 800$ GeV. For smaller compactification scales, one can always argue that any tiny negative boundary term correction to the $B^{(1)}$ mass will make the KK photon lighter³. Our guideline is phenomenology. The only interesting and plausible cases would correspond to the LKP being a neutral weakly interacting particle.

In the gauge boson sector, EWSB induces mixing between the gauge eigenstates, $B^{(1)}$ and $W_3^{(1)}$ in analogy with the familiar effect for the zero modes which produces the photon and Z boson. Including tree level contributions, EWSB effects, and radiative corrections to the masses, the mass matrix in the $(B^{(n)}, W_3^{(n)})$ basis is [21],

$$\begin{pmatrix} \frac{n^2}{R^2} + \frac{1}{4}g_1^2v^2 + \delta M_1^2 & \frac{1}{4}g_1g_2v^2 \\ \frac{1}{4}g_1g_2v^2 & \frac{n^2}{R^2} + \frac{1}{4}g_2^2v^2 + \delta M_2^2 \end{pmatrix}, \quad (2)$$

where g_1 and g_2 are the U(1) and SU(2) gauge couplings, respectively, $v \sim 174$ GeV is Higgs vacuum expectation value (VEV), R is the radius of the extra dimension, and δM_1^2 and δM_2^2 are the radiative corrections to the $B^{(1)}$ and $W^{(1)}$ masses, including the boundary terms. In the absence of the radiative corrections, the mixing between the KK gauge bosons would be the same as that for the zero modes, and one would have KK modes of the photon and Z with the same Weinberg angle as the zero modes. The radiative corrections will generally disrupt this relationship, and each KK level will generally have

³One might be worried about the late decay of the KK graviton into the LKP. Indeed we know that unstable TeV relics may be dangerous if their lifetime exceeds 10^6 s because of their effects on the primordially synthesized abundances of light elements. However, this is true for large relic densities. In the case of (massless as well as KK mode) gravitons, we expect a very suppressed relic number density because of their very weak coupling. On the other hand, theoretical predictions of relic gravitons are necessarily subject to large uncertainties. A reliable estimate is difficult to obtain since it depends on the complicated dynamics of preheating and on the specific inflationary model considered.

two neutral bosons which are different mixtures of $B^{(1)}$ and $W^{(1)}$. As explained above, from an effective theory point of view δM_1^2 and δM_2^2 are separate inputs for the UED theory, but it is self-consistent to imagine that they are small and the resulting corrections to the tree-level n/R masses are modest. Within this framework one could also imagine that it is natural to expect $\delta M_2^2 > \delta M_1^2$ because $g_2 > g_1$ and δM_2^2 is further enhanced by larger group factors. For simplicity, we work in the limit $\delta M_2^2 - \delta M_1^2 \gg g_1 g_2 v^2$, so the mixing angle is effectively driven to zero by the large diagonal entries in the mass matrix⁴. Within this framework, one expects the LKP to be well-approximated as entirely $B^{(1)}$. It thus couples to all SM fermions (and the Higgs) proportionally to their hypercharges with coupling g_1 , and is approximately decoupled from the gauge bosons.

Similar corrections apply to the Kaluza-Klein modes of the fermions, and generically their masses are also independent parameters of the theory. If one follows the prescription that the lightest particles are those which undergo only the U(1) hypercharge interaction, the lightest KK fermion would be the right-handed electron, $e_R^{(1)}$. Note that the subscript “R” refers to the fact that it is a KK mode of the right-handed electron (and thus is an SU(2) singlet) as opposed to its chirality; it is a massive Dirac fermion with both right- and left-handed polarizations. In Section 4, we consider the case in which $e_R^{(1)}$ is substantially heavier than $B^{(1)}$, and thus irrelevant in terms of its relic abundance while in Section 6.1, we also consider the case in which $e_R^{(1)}$ is only slightly heavier than $B^{(1)}$, and thus coannihilation effects can be significant. If one relaxes the restriction that the fields which experience the SU(2) interaction are heavier than those which only experience the U(1), one could also consider the $W_3^{(1)}$ or the $\nu^{(1)}$ as the LKP. We consider the case in which $\nu^{(1)}$ is the LKP, including a variety of coannihilation channels, in Section 5.

We continue to consider the zero mode gauge bosons in terms of their well-known mass eigenstates, γ , Z and W^\pm , however we simplify our results by neglecting all EWSB effects, which correct our results at most by $v^2 R^2$. Thus, we consider all of the SM fermions and gauge bosons as massless, and include the full content of the Higgs doublet (including the would-be Goldstone bosons) as massless physical degrees of freedom. This means that we neglect some processes, such as $B^{(1)} B^{(1)} \rightarrow$ zero mode gauge bosons all together, because they are $v^2 R^2$ suppressed compared to the dominant decay modes. It also means that we can choose to describe the neutral zero mode gauge bosons either in the $Z \gamma$ or in the $B^{(0)}, W_3^{(0)}$ basis, as is convenient for the problem at hand. This approximation will be further motivated below, where we find that the favored regions of parameter space for dark matter have the mass of the LKP on the order of 1 TeV, much greater than $v \sim 174$ GeV.

3 Density of a Cold Relic Particle

In this section, we review the standard calculation of the relic abundance of a particle species (see [25, 26] for more details) denoted \mathcal{Z} which was at thermal equilibrium in the

⁴This is not so different from the situation in [21], for which $\sin^2 \theta_W^{(1)} \lesssim 0.01$ for $1/R > 600$ GeV.

early universe and decoupled when it was non relativistic. The evolution of its number density n in an expanding universe is governed by the Boltzmann equation:

$$\frac{dn}{dt} + 3Hn = -\langle\sigma v\rangle (n^2 - n^{eq2}), \quad (3)$$

where $H = (8\pi\rho/3M_{Pl})^{1/2}$ is the expansion rate of the universe, n^{eq} the number density at thermal equilibrium and $\langle\sigma v\rangle$ is the thermally averaged annihilation cross section times the relative velocity. We are eventually concerned by a massive cold dark matter candidate, for which the equilibrium density is given by the non relativistic limit:

$$n^{eq} = g \left(\frac{mT}{2\pi}\right)^{3/2} e^{-m/T}, \quad (4)$$

where m is the mass of the particle species in question. The physics of equation (3) is the following: At early times, when the temperature was higher than the mass of the particle, the number density was $n^{eq} \propto T^3$, \mathcal{Z} annihilated with its own anti-particle into lighter states and *vice versa*. As the temperature decreased below the mass, n dropped exponentially as indicated in (4) and the annihilation rate $\Gamma = n\langle\sigma v\rangle$ dropped below H . The \mathcal{Z} particles can no longer annihilate and their density per comoving volume remains fixed. The temperature at which the particle decouples from the thermal bath is denoted T_F (*freeze-out temperature*) and roughly corresponds to the time when Γ is of the same order as H .

Equation (3) can be rewritten in terms of the variable $Y = n/s$, $Y^{eq} = n^{eq}/s$ where s is the entropy $s = 2\pi^2 g_* T^3/45$. g_* counts the number of relativistic degrees of freedom. From the conservation of entropy per comoving volume ($sa^3 = \text{constant}$) we get $\dot{n} + 3Hn = s\dot{Y}$ so that

$$s\dot{Y} = -\langle\sigma v\rangle s^2 (Y^2 - Y^{eq2}). \quad (5)$$

We now introduce the variable:

$$x = \frac{m}{T}. \quad (6)$$

In a radiation dominated era,

$$H^2 = \frac{4\pi^3 g_* T^4}{45 M_{Pl}^2}, \quad t = \frac{1}{2H} \quad \rightarrow \quad \frac{dx}{dt} = Hx, \quad (7)$$

and (5) reads:

$$\frac{dY}{dx} = -\frac{\langle\sigma v\rangle}{Hx} s (Y^2 - Y^{eq2}). \quad (8)$$

As is well known, $\langle\sigma v\rangle$ is well approximated by a non relativistic expansion (obtained by replacing the square of the energy in the center of mass frame by $s = 4m^2 + m^2 v^2$):

$$\langle\sigma v\rangle = a + b\langle v^2\rangle + \mathcal{O}(\langle v^4\rangle) \approx a + 6 b/x. \quad (9)$$

We finally rewrite our master equation (8) in terms of the variable $\Delta = Y - Y^{eq}$:

$$\Delta' = -Y^{eq'} - f(x)\Delta(2Y^{eq} + \Delta), \quad (10)$$

where

$$f(x) = \sqrt{\frac{\pi g_*}{45}} m M_{Pl} (a + 6 b/x) x^{-2}. \quad (11)$$

A simple analytic solution can be obtained by studying this equation in two extreme regimes. At very early times when $x \ll x_F = m/T_F$, $\Delta' \ll Y^{eq'}$ and Δ is given by:

$$\Delta = -\frac{Y^{eq'}}{f(x)(2Y^{eq} + \Delta)}. \quad (12)$$

At late times, $\Delta \sim Y \gg Y^{eq}$ and $\Delta' \gg Y^{eq'}$ leading to

$$\Delta^{-2} \Delta' = -f(x). \quad (13)$$

Integrating this equation between x_F and ∞ and using the fact that $\Delta_{x_F} \gg \Delta_\infty$:

$$\Delta_\infty = \frac{1}{\int_{x_F}^{\infty} f(x) dx} \approx Y_\infty. \quad (14)$$

We arrive at:

$$Y_\infty^{-1} = \sqrt{\frac{\pi g_*}{45}} M_{Pl} m x_F^{-1} (a + 3b/x_F). \quad (15)$$

The contribution of the \mathcal{Z} particle to the energy density of the universe is given by

$$\Omega_{\mathcal{Z}} = \rho_{\mathcal{Z}}/\rho_c, \quad (16)$$

where ρ_c is the critical density corresponding to a flat universe,

$$\rho_c = 3H_0^2 M_{Pl}^2/8\pi = 1.0539 \times 10^{-5} h^2 \text{GeV cm}^{-3}, \quad (17)$$

The value for h is given in equation (1). $\rho_{\mathcal{Z}}$ is simply given by $\rho_{\mathcal{Z}} = m_{\mathcal{Z}} n_{\mathcal{Z}} = m_{\mathcal{Z}} s_0 Y_\infty$, $s_0 = 2889.2 \text{ cm}^{-3}$ being the entropy today. Finally, the contribution to Ω from a given non relativistic species of mass $m_{\mathcal{Z}}$ is:

$$\Omega_{\mathcal{Z}} h^2 \approx \frac{1.04 \times 10^9}{M_{Pl}} \frac{x_F}{\sqrt{g_*}} \frac{1}{(a + 3b/x_F)}, \quad (18)$$

where g_* is evaluated at the freeze-out temperature. For our cases of interest, we will have freeze-out temperatures in the region of 50 GeV, for which we use $g_* = 92$. Note that the mass $m_{\mathcal{Z}}$ does not appear explicitly in this expression. Its effect is hidden in the coefficients a and b (of dimension GeV^{-2}) as well as x_F . Therefore, all we have to do is to compute the annihilation cross sections, expand them in the non relativistic limit and extract the coefficients a and b . We must also determine x_F , the freeze-out temperature.

The freeze-out temperature is defined by solving the equation

$$\Delta(x_F) = c Y^{eq}(x_F), \quad (19)$$

using the expression for $\Delta(x)$ at early times. c is a constant of order one determined by matching the late-time and early-time solutions. It can be chosen empirically by comparing to a numerical integration of the Boltzmann equation. Equation (19) leads to

$$x_F = \ln \left(c(c+2) \sqrt{\frac{45}{8}} \frac{g}{2\pi^3} \frac{m M_{Pl}(a + 6b/x_F)}{g_*^{1/2} x_F^{1/2}} \right) \quad (20)$$

which is solved iteratively. The result does not depend dramatically on the precise value of c which we will take to have the usual value $c = 1/2$.

3.1 Including Coannihilation

As pointed out in [26], the derivation presented above needs to be readdressed in the case of coannihilation. Here, we briefly summarize the approach presented in [26] to be followed in this case. Such situation occurs when there are particles nearly degenerate with the relic \mathcal{Z} but with masses slightly greater than $m_{\mathcal{Z}}$. These extra particles are nearly abundant as \mathcal{Z} and if the mass difference is smaller or of the same order as the temperature when \mathcal{Z} freezes out, they are thermally accessible and their annihilation will play a major role in determining the relic abundance of \mathcal{Z} . Let us label \mathcal{Z}_i , $i = 1, \dots, N$, these particles nearly degenerate in mass. \mathcal{Z}_1 is the LKP, \mathcal{Z}_2 is the next LKP, *etc.* We also denote X, X' any zero mode (SM) particles. Reactions such as $\mathcal{Z}_i \mathcal{Z}_j \leftrightarrow XX'$ change the \mathcal{Z}_i densities n_i and determine their abundances. Since all $\mathcal{Z}_{i>1}$ which survive annihilation eventually decay into \mathcal{Z}_1 , the relevant quantity is the total density of \mathcal{Z}_i particles $n = \sum_{i=1}^N n_i$, and the Boltzmann equation for n can be rewritten with accurate approximation as [26]:

$$\frac{dn}{dt} = -3Hn - \langle \sigma_{\text{eff}} v \rangle (n^2 - n^{eq2}), \quad (21)$$

where

$$\sigma_{\text{eff}} = \sum_{ij} \sigma_{ij} \frac{g_i g_j}{g_{\text{eff}}^2} (1 + \Delta_i)^{3/2} (1 + \Delta_j)^{3/2} e^{-x(\Delta_i + \Delta_j)}. \quad (22)$$

σ_{ij} is the cross section for the reaction $\mathcal{Z}_i \mathcal{Z}_j \rightarrow XX'$, g_i is the number of degrees of freedom of \mathcal{Z}_i , $\Delta_i = (m_i - m_1)/m_1$, and,

$$g_{\text{eff}} = \sum_i^N g_i (1 + \Delta_i)^{3/2} e^{-x\Delta_i}. \quad (23)$$

Equation (21) is of the same form as (3) and can be solved using similar techniques. The formula for x_F becomes,

$$x_F = \ln \left(c(c+2) \sqrt{\frac{45}{8}} \frac{g_{\text{eff}}}{2\pi^3} \frac{m M_{Pl}(a_{\text{eff}} + 6b_{\text{eff}}/x_F)}{g_*^{1/2} x_F^{1/2}} \right), \quad (24)$$

where g has been replaced by g_{eff} and a and b by a_{eff} and b_{eff} , the coefficients of the Taylor expansion for σ_{eff} . The relic abundance now reads:

$$\Omega_{\mathcal{Z}_1} h^2 = \frac{1.04 \times 10^9 \text{ GeV}^{-1} x_F}{g_*^{1/2} M_{Pl} (I_a + 3I_b/x_f)}, \quad (25)$$

with

$$I_a = x_F \int_{x_F}^{\infty} a_{\text{eff}} x^{-2} dx, \quad \text{and} \quad I_b = 2x_F^2 \int_{x_F}^{\infty} b_{\text{eff}} x^{-3} dx. \quad (26)$$

We now apply this formalism to our dark matter candidates. As explained in section II, we will consider both cases $\mathcal{Z}_1 = B^{(1)}$ and $\mathcal{Z}_1 = \nu^{(1)}$. We have computed the annihilation cross sections of the LKP into any zero mode (SM) particle. We begin by ignoring coannihilation and focus on the $B^{(1)}$ and $\nu^{(1)}$ candidates. Coannihilation effects will be considered in section 6.

4 $B^{(1)}$ as the LKP without Coannihilation

We now analyze the case in which the LKP is $B^{(1)}$, and all other KK modes are considerably heavier (roughly 10% or more [26]), so they do not play a significant role in the final relic density of the $B^{(1)}$. The relevant cross sections for pairs of $B^{(1)}$ to annihilate have final states into fermions or into Higgs bosons. In the limit in which EWSB effects are neglected, there are no channels into vector bosons. For simplicity, we neglect the mass splittings between the LKP and the higher states in the cross sections, expressions for which may be found in Appendix A.

From these cross sections, we derive the coefficients in the thermal average discussed above, finding,

$$a = \frac{4\pi\alpha_1^2 (2Y_F + 3Y_H)}{9m_{KK}^2},$$

$$b = -\frac{\pi\alpha_1^2 (2Y_F + 3Y_H)}{18m_{KK}^2}, \quad (27)$$

where $Y_F = 95/18$ and $Y_H = 1/16$. Numerically, for $m_{KK} = 1$ TeV, the effective annihilation cross section is $\sigma \sim 0.6$ pb, and the annihilation is 35% into quark pairs, 59% into charged lepton pairs, 4% into neutral leptons, and 2% into Higgs. For different masses, the cross section falls as m_{KK}^{-2} and the relative importance of the various final states stays approximately constant. As discussed above, these results allow us to determine x_F , and we find that it is a very slowly varying function of m_{KK} , decreasing from $x_F = 26$ for $m_{KK} = 200$ GeV to $x_F = 24$ for $m_{KK} = 2$ TeV. Therefore, it is essentially a and b which control the m_{KK} dependence of $\Omega_{B^{(1)}}$.

In Figure 1 we present the prediction for $\Omega_{B^{(1)}} h^2$ as a function of the KK mass for five dimensions. In five dimensions, an upper bound $m_{KK} \lesssim 1.9$ TeV is set from the universe overclosure condition and to account for the dark matter ($\Omega = 0.33 \pm 0.035$), we find

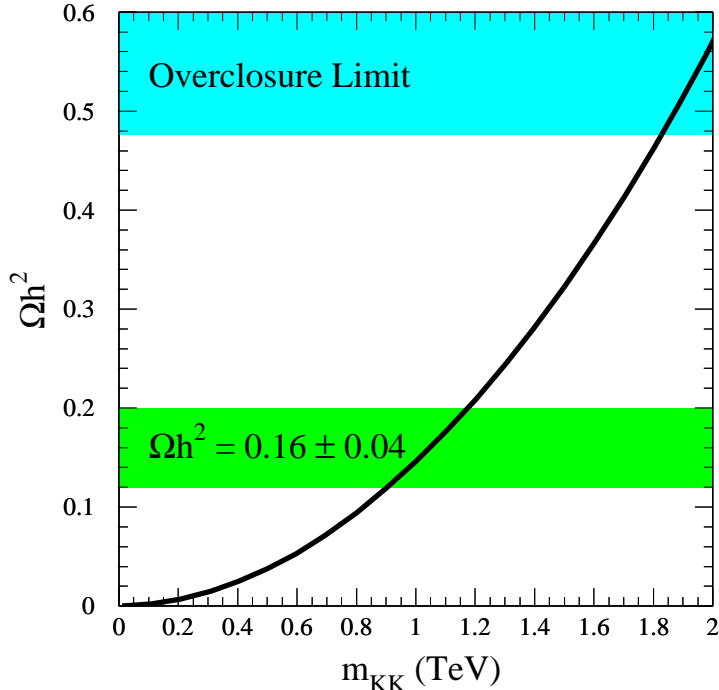


Figure 1: Prediction for $\Omega_{B^{(1)}}h^2$ as a function of the KK mass (when neglecting coannihilation). The upper horizontal region delimits the values of Ωh^2 above which the contribution from $B^{(1)}$ to the energy density would overclose the universe. The lower horizontal band denotes the region $\Omega = 0.33 \pm 0.035$ (using $h = 0.69 \pm 0.06$) and defines the KK mass window if all the dark matter is to be accounted for by the $B^{(1)}$ LKP.

that the KK mass must lie in the range $m_{KK} \sim 900 - 1200$ GeV, with a corresponding freeze-out temperature of order $T_F \sim 36 - 48$ GeV. These results are slightly above the experimental bounds on universal extra dimensions from precision electroweak data and collider searches (~ 350 GeV for one extra dimension [5]), and imply that provided the fermion KK modes are not very much heavier than the $B^{(1)}$, future collider experiments will be able to study the region relevant for dark matter.

5 $\nu^{(1)}$ without Coannihilation

The situation is slightly more intricate in the case where the neutrino is the LKP. To begin with, we now have a relic density composed of both the $\nu^{(1)}$ and its anti-particle, both of which annihilate among themselves as well as with each other. We assume that there is no cosmic asymmetry between particle and anti-particle in the analysis below.

If there were a large asymmetry generated before freeze-out, this effect could dominate the eventual relic abundance, and the computation below would have to be modified. We must also consider a larger number of annihilation processes, including final states of fermions, Higgs, and Z and W^\pm gauge bosons. The various channels are listed in Appendix B along with the necessary cross section formulae.

We continue to consider the regime in which the other KK modes are considered light enough that we can neglect the mass splittings in the cross sections, but heavy enough that they do not result in a large modification of the final relic density. One would naturally expect the mass of the $e_L^{(1)}$ to be close to $\nu^{(1)}$, its weak partner. In fact any mass splitting between the two KK modes is an effect of EWSB, and could lead to dangerously large contributions to the T parameter [27]. Such a contribution could be compensated by, *i.e.* a heavy Higgs boson [28]. As we will see below in Section 6.2, including a degenerate $e_L^{(1)}$ will not substantially alter our results.

5.1 One Flavor

Our relic density is both $\nu^{(1)}$ and $\bar{\nu}^{(1)}$ ($n_{\mathcal{Z}} = n_{\nu^{(1)}} + n_{\bar{\nu}^{(1)}}$ with $g_{\text{eff}} = 4$) so that the annihilation cross section appearing in the Boltzmann equation is

$$\sigma_{\text{eff}} = \frac{1}{4} \left[\sigma(\nu^{(1)}\nu^{(1)} \rightarrow \nu\nu) + \sigma(\bar{\nu}^{(1)}\bar{\nu}^{(1)} \rightarrow \bar{\nu}\bar{\nu}) + 2 \sigma(\nu^{(1)}\bar{\nu}^{(1)} \rightarrow X) \right], \quad (28)$$

with

$$\begin{aligned} \sigma(\nu^{(1)}\bar{\nu}^{(1)} \rightarrow X) &= \sigma(\nu^{(1)}\bar{\nu}^{(1)} \rightarrow q\bar{q}) + \sigma(\nu^{(1)}\bar{\nu}^{(1)} \rightarrow \nu\bar{\nu}) + \sigma(\nu^{(1)}\bar{\nu}^{(1)} \rightarrow l^+l^-) \\ &+ \sigma(\nu^{(1)}\bar{\nu}^{(1)} \rightarrow ZZ) + \sigma(\nu^{(1)}\bar{\nu}^{(1)} \rightarrow W^+W^-) \\ &+ \sigma(\nu^{(1)}\bar{\nu}^{(1)} \rightarrow \phi\phi^*), \end{aligned} \quad (29)$$

where the cross section into quarks contains a sum over all quark flavors, the cross section into neutrinos contains a sum into both the neutrino zero mode of $\nu^{(1)}$ and the other flavors, and the cross section into charged leptons includes both the zero mode charged partner of $\nu^{(1)}$, and also the other flavors. Note that the matrix elements for annihilation into other flavors are different from those into zero modes of the same flavor.

Proceeding as before, we expand the effective cross section in powers of $1/x_F$, obtaining,

$$\begin{aligned} a_{\text{eff}} &= \frac{\alpha^2\pi (272s_W^4 - 281s_W^2 + 154)}{192s_W^4 c_W^4 m_{KK}^2} \\ b_{\text{eff}} &= -\frac{\alpha^2\pi (274s_W^4 - 127s_W^2 + 4)}{1536s_W^4 c_W^4 m_{KK}^2} \end{aligned} \quad (30)$$

where the $\nu\bar{\nu}$ portion of the result sums over all allowed final states, including 3 up- and down-type quarks, 3 charged and neutral leptons, ZZ and W^+W^- weak bosons, and the Higgs doublet. For $m_{KK} = 1$ TeV, we have the effective cross section $\sigma_{\text{eff}} = 1.3$ pb, slightly

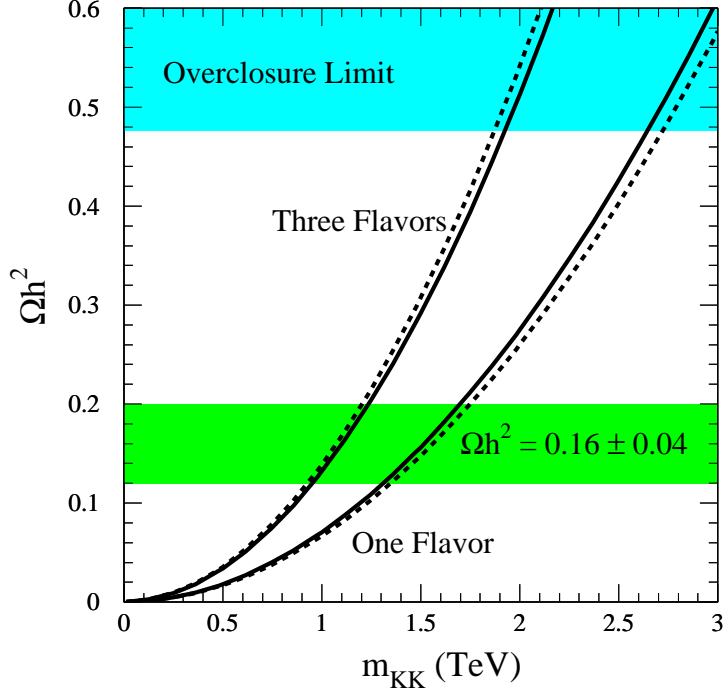


Figure 2: Prediction for $\Omega_{\nu^{(1)}} h^2$ as a function of the KK mass. The solid lines are for $\nu^{(1)}$ alone (in the one and three family cases) and the dotted ones correspond to the cases where coannihilation with degenerate $e_L^{(1)}$ is included.

higher than the $B^{(1)}$ case. σ_{eff} is composed 18% of the process $\nu^{(1)}\nu^{(1)} \rightarrow \nu\nu$, with the remaining 82% coming from $\nu^{(1)}\bar{\nu}^{(1)} \rightarrow X$. This second contribution is roughly 41% into quarks, 7% / 9% into neutral/charged gauge bosons, 2% into Higgs, and 33% / 8% into charged/neutral leptons.

Deriving the freeze-out temperature, we find that x_F varies from 27 for $m_{KK} = 0.2$ TeV to 25 for $m_{KK} = 2$ TeV. $\nu^{(1)}$ therefore freezes out somewhat later than $B^{(1)}$ and thus has a smaller relic density. The higher effective annihilation cross section translates into a different prediction for the KK mass to account for the dark matter energy density: $m_{KK} \sim 1.3 - 1.8$ TeV and the overclosure limit is pushed up to 2.7 TeV (see figure 2). Again, these values are within the reach of planned experiments such as the LHC, provided the colored KK mode masses are not significantly different from the mass of the KK neutrino. The value for x_F is not much different from the $B^{(1)}$ case, however, given the different m_{KK} window, the freeze-out temperature is higher, $T_F \sim 50 - 70$ GeV.

5.2 Three Flavors

If we consider three degenerate flavors of KK neutrino, the relic density is computed as the sum of the densities of all three species plus the sum of the corresponding anti-particles. Thus we have $g_{\text{eff}} = 12$. In this case, the effective cross section contains three separate contributions identical to that considered above, for each species to annihilate among itself, and also additional cross-flavor channels such as $\nu_1^{(1)}\nu_2^{(1)} \rightarrow \nu_1\nu_2$, $\nu_1^{(1)}\bar{\nu}_2^{(1)} \rightarrow \nu_1\bar{\nu}_2$, etc through t -channel $Z^{(1)}$ exchange. There are also cross-flavor transitions into charged leptons through t -channel $W_{\pm}^{(1)}$ exchange. The relevant formulae may be found in Appendix B. We continue to assume no cosmological asymmetries between particles and anti-particles, and further consider the case where there are no asymmetries between different flavors.

The effective cross section becomes,

$$\begin{aligned} \sigma_{\text{eff}} = & \frac{1}{12} \left[\sigma(\nu_1^{(1)}\nu_1^{(1)} \rightarrow \nu_1\nu_1) + \sigma(\bar{\nu}_1^{(1)}\bar{\nu}_1^{(1)} \rightarrow \bar{\nu}_1\bar{\nu}_1) + 2\sigma(\nu_1^{(1)}\bar{\nu}_1^{(1)} \rightarrow X) \right. \\ & \left. + 2\sigma(\nu_1^{(1)}\nu_2^{(1)} \rightarrow \nu_1\nu_2) + 2\sigma(\bar{\nu}_1^{(1)}\bar{\nu}_2^{(1)} \rightarrow \bar{\nu}_1\bar{\nu}_2) + 4\sigma(\nu_1^{(1)}\bar{\nu}_2^{(1)} \rightarrow X) \right] \quad (31) \end{aligned}$$

where we have assumed that cross sections for all flavors (and combinations of flavors) are equal. The cross-flavor annihilation channels are not as efficient as the same-flavor channels (about twice in size), and x_F is about the same as in the single flavor case. Thus, the net result is a larger predicted relic abundance for the same mass, as shown in Figure 2. Thus, the region relevant to explain measurements is lower, $m_{KK} \sim 950 - 1250$ GeV, and the overclosure condition requires $m_{KK} \lesssim 1.9$ TeV. The freeze-out temperature in the relevant region ranges from 36 – 47 GeV.

6 Coannihilation Results

Coannihilation is expected to play a significant role when there are extra degrees of freedom with masses nearly degenerate with the relic particle. Experience with the supersymmetric standard model indicates that large effects are to be expected when the heavier particles have masses within about 5% of the LSP. The radiative corrections to the KK spectrum under the prescription of Ref. [21] indicate that quark and gluon KK masses can be shifted by twenty percents. Weak gauge bosons also receive corrections (at tree level) larger than five percents so that the only particles which will be considered as nearly degenerate with the LKP are the leptons. We will simplify our analysis by considering all higher Kaluza-Klein modes relevant for coannihilation to be degenerate, and leave the splitting between the LKP and next lightest Kaluza-Klein particle (NLKP) as an adjustable parameter.

As motivated in Section 2, we will compute coannihilation channels in the two following situations:

- $B^{(1)}$ is the LKP and $e_R^{(1)}$ is the NLKP with all other KK modes heavy enough that they do not contribute to coannihilation,

- $\nu^{(1)}$ is the LKP and $e_L^{(1)}$ is the NLKP (almost degenerate).

The relative mass difference between the LKP and the second LKP is denoted by $\Delta = (m_{NLKP} - m_{LKP})/m_{LKP}$.

6.1 $B^{(1)}$ Coannihilation with $e_R^{(1)}$

In the first case, we consider $B^{(1)}$ as the LKP and $e_R^{(1)}$ as the NLKP, assuming no net asymmetry between the number of $e_R^{(1)}$ and $\bar{e}_R^{(1)}$. We consider both the case with one family of $e_R^{(1)}$, and also the case of three degenerate families. With one family, the formula (23) for the effective number of degrees of freedom becomes,

$$g_{\text{eff}} = 3 + 4(1 + \Delta)^{3/2} \exp[-x\Delta], \quad (32)$$

where we have used $g_f = 2, g_{B^1} = 3$ and summed over $B^{(1)}, \nu^{(1)}$, and $\bar{\nu}^{(1)}$. The effective annihilation cross section is,

$$\begin{aligned} g_{\text{eff}}^2 \sigma_{\text{eff}} &= g_{B^1}^2 \sigma(B^{(1)}B^{(1)}) + 4g_{B^1} g_f [1 + \Delta]^{3/2} \exp[-x\Delta] \sigma(B^{(1)}e_R^{(1)}) \\ &\quad + 2g_f^2 [1 + \Delta]^3 \exp[-2\Delta x] \left(\sigma(e_R^{(1)}e_R^{(1)}) + \sigma(e_R^{(1)}\bar{e}_R^{(1)}) \right), \end{aligned} \quad (33)$$

where we have assumed that the cross sections for annihilation of $(B^{(1)}e_R^{(1)}, B^{(1)}\bar{e}_R^{(1)})$ and $(e_R^{(1)}e_R^{(1)}, \bar{e}_R^{(1)}\bar{e}_R^{(1)})$ into zero modes are equal.

The cross section $\sigma(B^{(1)}B^{(1)})$ is as derived before in Section 4. The cross section $\sigma(B^{(1)}e_R^{(1)})$ proceeds into final states with zero modes of $e\gamma$ and eZ , and in the limit in which the Z mass is neglected can be equivalently described as a single process $e_R^{(1)}B^{(1)} \rightarrow eB^{(0)}$. No νW^- final state occurs because $e_R^{(1)}$, being a weak singlet, does not couple to the $SU(2)$ bosons, and we neglect the tiny electron Yukawa coupling which would result in a $e\Phi^0$ final state. There are also channels which convert $e_R^{(1)}\bar{e}_R^{(1)}$ into fermions and Higgs through an s -channel $B^{(0)}$ and into two $B^{(0)}$'s (or equivalently, into $ZZ, \gamma\gamma$ and $Z\gamma$ final states); and channels in which $e_R^{(1)}e_R^{(1)}$ exchanges a $B^{(1)}$ to become lepton zero modes. If more than one flavor of $e_R^{(1)}$ has a mass close to $B^{(1)}$, one also has channels in which different flavors of $e_R^{(1)}$ exchange a t -channel $B^{(1)}$ and thus scatter into their corresponding zero modes. All of the needed cross sections are given in Appendix C.

Our result when including $e_R^{(1)}$ almost degenerate with $B^{(1)}$ ($\Delta = 1\%$) is a higher LKP relic density than in the case without $e_R^{(1)}$. Indeed, the self annihilation cross section of $e_R^{(1)}$ is not much higher than the one for $B^{(1)}$ and the coannihilation cross section is significantly smaller (there are only two coannihilation channels while $B^{(1)}$ and $e_R^{(1)}$ can self annihilate into all zero mode fermions). This situation is to be contrasted with the SUSY case where coannihilation between the neutralino and sfermions can be very efficient and significantly reduce the relic density. Here, we have more relics (both $B^{(1)}$ and $e_R^{(1)}$) which essentially decoupled at the same time (and at roughly the same freeze-out temperature as was the case for $B^{(1)}$ alone) and eventually the left over $e_R^{(1)}$ decay into $B^{(1)}$. This

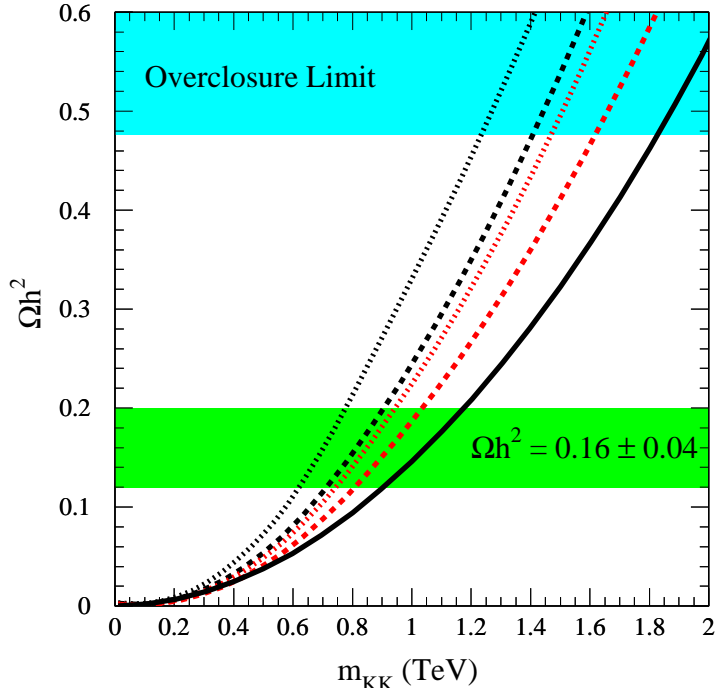


Figure 3: Prediction for $\Omega_{B^{(1)}}h^2$ as in Figure 1. The solid line is the case for $B^{(1)}$ alone, and the dashed and dotted lines correspond to the case in which there are one (three) flavors of nearly degenerate $e_R^{(1)}$. For each case, the black curves (upper of each pair) denote the case $\Delta = 0.01$ and the red curves (lower of each pair) $\Delta = 0.05$.

translates into a KK mass window slightly below the window obtained for $B^{(1)}$ alone. In Figure 3 we present the resulting relic abundance of $B^{(1)}$ including both the one flavor and three flavors of $e_R^{(1)}$, for two choices of Δ corresponding to 1% and 5% mass splittings. The curves become approximately degenerate with the $B^{(1)}$ without coannihilation case when $\Delta \gtrsim 0.1$. In each case, the resulting m_{KK} window shifts slightly downward because of the increase in the predicted relic density, favoring values between 600 – 1050 GeV, depending on the number of light $e_R^{(1)}$ flavors and the mass splitting.

6.2 $\nu^{(1)}$ Coannihilation with $e_L^{(1)}$

As mentioned in the introduction of section 5, one should include $e_L^{(1)}$ in the calculation of the LKP relic density when assuming that the LKP is $\nu^{(1)}$. Indeed, $\nu^{(1)}$ and $e_L^{(1)}$ are expected to be nearly degenerate, with tree level mass splittings on the order of the mass

of the charged lepton. For one family of leptons we have,

$$g_{\text{eff}} = 4 + 4(1 + \Delta)^{3/2} \exp[-x\Delta], \quad (34)$$

and the effective annihilation cross section is:

$$\begin{aligned} g_{\text{eff}}^2 \sigma_{\text{eff}} = & g_f^2 \left\{ 2\sigma(\nu^{(1)}\nu^{(1)} \rightarrow \nu\nu) + 2\sigma(\nu^{(1)}\bar{\nu}^{(1)} \rightarrow X) \right. \\ & + \left[2\sigma(e_L^{(1)}e_L^{(1)} \rightarrow e^-e^-) + 2\sigma(e_L^{(1)}\bar{e}_L^{(1)} \rightarrow X) \right] (1 + \Delta)^3 e^{-2\Delta x} \\ & \left. + \left[4\sigma(\nu^{(1)}e_L^{(1)} \rightarrow \nu e^-) + 4\sigma(e_L^{(1)}\bar{\nu}^{(1)} \rightarrow X) \right] (1 + \Delta)^{3/2} e^{-x\Delta} \right\} \end{aligned} \quad (35)$$

where,

$$\begin{aligned} \sigma(e_L^{(1)}\bar{e}_L^{(1)} \rightarrow X) = & \sigma(e_L^{(1)}\bar{e}_L^{(1)} \rightarrow q\bar{q}) + \sigma(e_L^{(1)}\bar{e}_L^{(1)} \rightarrow \nu\bar{\nu}) + \sigma(e_L^{(1)}\bar{e}_L^{(1)} \rightarrow l^+l^-) \\ & + \sigma(e_L^{(1)}\bar{e}_L^{(1)} \rightarrow ZZ, Z\gamma, \gamma\gamma) + \sigma(e_L^{(1)}\bar{e}_L^{(1)} \rightarrow W^+W^-) \\ & + \sigma(e_L^{(1)}\bar{e}_L^{(1)} \rightarrow \phi\phi^*), \end{aligned} \quad (36)$$

$$\begin{aligned} \sigma(e_L^{(1)}\bar{\nu}^{(1)} \rightarrow X) = & \sigma(e_L^{(1)}\bar{\nu}^{(1)} \rightarrow q\bar{q}') + \sigma(e_L^{(1)}\bar{\nu}^{(1)} \rightarrow e^-\bar{\nu}) + \\ & + \sigma(e_L^{(1)}\bar{\nu}^{(1)} \rightarrow W^-Z) + \sigma(e_L^{(1)}\bar{\nu}^{(1)} \rightarrow W^+\gamma) \\ & + \sigma(e_L^{(1)}\bar{\nu}^{(1)} \rightarrow \phi\phi^*). \end{aligned} \quad (37)$$

For the three family case, we also include the cross flavor annihilation channels,

$$g_{\text{eff}} = 12 + 12(1 + \Delta)^{3/2} \exp[-x\Delta], \quad (38)$$

and,

$$\begin{aligned} g_{\text{eff}}^2 \sigma_{\text{eff}} = & 3g_f^2 \left\{ 2\sigma(\nu^{(1)}\nu^{(1)} \rightarrow \nu\nu) + 2\sigma(\nu^{(1)}\bar{\nu}^{(1)} \rightarrow X) \right. \\ & + 4\sigma(\nu_1^{(1)}\nu_2^{(1)} \rightarrow \nu_1\nu_2) + 4\sigma(\nu_1^{(1)}\bar{\nu}_2^{(1)} \rightarrow X) \\ & + \left[2\sigma(e_L^{(1)}e_L^{(1)} \rightarrow e^-e^-) + 2\sigma(e_L^{(1)}\bar{e}_L^{(1)} \rightarrow X) \right. \\ & \left. + 4\sigma(e_L^{(1)}\mu_L^{(1)} \rightarrow e^-\mu^-) + 4\sigma(\bar{e}_L^{(1)}\mu_L^{(1)} \rightarrow X) \right] (1 + \Delta)^3 e^{-2\Delta x} \\ & + \left[4\sigma(\nu^{(1)}e_L^{(1)} \rightarrow \nu e^-) + 4\sigma(e_L^{(1)}\bar{\nu}^{(1)} \rightarrow X) \right. \\ & \left. + 4\sigma(\mu_L^{(1)}\bar{\nu}^{(1)} \rightarrow \mu^-\bar{\nu}) + 4\sigma(\mu_L^{(1)}\nu^{(1)} \rightarrow X) \right] (1 + \Delta)^{3/2} e^{-x\Delta} \left. \right\}, \end{aligned} \quad (39)$$

with,

$$\sigma(\bar{e}_L^{(1)}\mu_L^{(1)} \rightarrow X) = \sigma(\bar{e}_L^{(1)}\mu_L^{(1)} \rightarrow e^+\mu^-) + \sigma(\bar{e}_L^{(1)}\mu_L^{(1)} \rightarrow \bar{\nu}_e\nu_\mu), \quad (40)$$

$$\sigma(\mu_L^{(1)}\nu^{(1)} \rightarrow X) = \sigma(\mu_L^{(1)}\nu^{(1)} \rightarrow \mu^-\nu) + \sigma(\mu_L^{(1)}\nu^{(1)} \rightarrow \nu_\mu e^-). \quad (41)$$

All relevant cross sections are given in Appendix C. From these results, we derive the freeze-out temperature and final relic density as a function of the mass splitting, $\Delta = (m_{e_L^{(1)}} - m_{\nu^{(1)}})/m_{\nu^{(1)}}$. We find that the result when $\Delta = 0$ is a small modification of that with $\nu^{(1)}$ alone. The modification of the freeze-out temperature is less than 1% over the relevant mass range, and the final relic density, shown in Figure 2, is slightly decreased in the one family case and increased in the three family case. As Δ increases, the results rapidly return to the corresponding $\nu^{(1)}$ results.

7 Summary and open questions

In this work, we have computed the contribution to the energy density of the Universe coming from the relic density of the Lightest Kaluza–Klein Particle in two cases: 1) The LKP is a Kaluza–Klein photon, 2) the LKP is a Kaluza–Klein neutrino. In models with universal extra dimensions (UED), such particle is stable and provides an interesting Dark Matter candidate whose mass is the inverse of the compactification radius⁵ R . One could question under which general conditions is the KK parity preserved. There can indeed be violations of KK parity because of the states and interactions which are localized at the two orbifold fixed points. However, if the boundary Lagrangians are symmetric under interchange of the two boundaries, KK parity will be preserved and unaltered by radiative corrections. The boundary Lagrangian describing any coupling between states localized at the boundaries and bulk fields is invariant under KK parity when fields and couplings are the same at the two fixed points. In a string theory context, couplings between bulk modes and twisted sectors can be predicted. While the symmetry of the boundary Lagrangians is not generic, it is not either disfavoured and it is not difficult to imagine string theories which could preserve KK parity and still have all of the features necessary. The assumption that KK parity is preserved does not conflict decisively with any feature that a low energy theory derived from string theory must possess.

We have assumed for simplicity that the Standard Model lives 4+1 dimensions. One could generalize our results to a higher number of extra dimensions⁶. The generalization to the six-dimensional case is reasonably straightforward. Let us consider for simplicity two extra dimensions with the topology of a torus, and equal radii. We impose either a \mathcal{Z}_2 or \mathcal{Z}_4 orbifold symmetry, so our spaces are T^2/\mathcal{Z}_2 and T^2/\mathcal{Z}_4 . For T^2/\mathcal{Z}_2 our particles have now two KK numbers and there are two LKP degenerate in mass: $B^{(1,0)}$ and $B^{(0,1)}$ and two heavier stable states, $B^{(1,1)}$ and $B^{(1,-1)}$ whose tree-level masses are about 40% larger. Following the formalism developed in Section 3.1, we see that for such large mass splittings, we expect the contribution of the heavier stable states to Ω_M to be exponentially suppressed compared to the light states, and thus we neglect them in the analysis. Because of KK number conservation (mod 2), at tree level the two LKP do not talk to each other and annihilate independently. The number of zero modes remains the same, therefore the relic density is just twice the one computed in the 5D case. The KK mass window to account for the DM is shifted to 650-850 GeV and the limit for overclosure is 1.3 TeV. For T^2/\mathcal{Z}_4 there are two stable particles with KK numbers (0, 1) and (1, 1). Again, the heavier state has a tree level mass about 40% heavier than the LKP, and we thus conclude that the prediction for Ω_M is approximately the same as the 5d case. The generalization to seven or more dimensions is more subtle because the number of

⁵ Note that in models with TeV compactification scale, the higher dimensional Planck scale is $\sim 10^{14}$ GeV for one extra dimension and $\sim 10^{11}$ GeV for two extra dimensions.

⁶One should also keep in mind that the computation of the relic density is a sensitive function of the expansion rate of the universe. The standard calculation assumes that the expansion rate is given by the conventional Friedmann equation evaluated in a radiation-dominated era corresponding to universe made of a gas of relativistic SM particles. Any deviation from this assumption will affect the relic density.

fermionic degrees of freedom is modified. One advantage of this model is that the physics is dominated by a single parameter: the size of the extra dimension, R . Interestingly, for the UED model to explain the Dark Matter with the LKP, we find that R typically has to be of the TeV scale, which is phenomenologically interesting and relevant at future colliders.

Having checked that the prediction for Ω_M is of the right order, the next step is to consider detection. Similarly to other WIMPs, the direct search for the LKP relies on the deposition of \sim keV recoil energy when the WIMP scatters from a nucleus in a detector. To study in more details the constraints on the LKP as the dark matter, the computation of the corresponding elastic scattering cross section between $B^{(1)}$ (or $\nu^{(1)}$) and a nucleus is needed. This task is beyond the aim of this paper. In addition, indirect WIMP searches rely on the detection of γ rays, charged particles or neutrinos from WIMP annihilation. There are two places where annihilation can take place:

- In the Sun where the LKP may be captured and annihilation greatly enhanced. This will generate a neutrino spectrum. The prediction essentially depends on the competition between the gravitational capture of the LKP by the Sun and the LKP annihilation so we would need to know the details of the capture rates and of the propagation of the neutrinos from the core to the surface of the Sun to make any statement.
- In the core of the Milky Way. LKP annihilation is important in the galactic center where the matter density is higher. To compute the resulting spectrum, one needs to know the reprocessing of the direct products of LKP annihilation.

Among secondary products of annihilation in the galactic center are high energy γ originating via neutral pion decays (pions result from the hadronization of the directly produced quarks) and the synchrotron radiation of e^+e^- pairs originating from the decays of charged pions in the galactic magnetic field. This requires the implementation of fragmentation functions. However, the flux of neutrinos coming from the direct LKP annihilation in the galactic center can be determined reasonably model-independently. These neutrinos will not be reprocessed during their journey between the galactic center and us. To do that, we use a Navarro–Frenk–White profile for the Milky Way of the form:

$$\rho_{dm}(r) = \rho_0 \frac{R_0}{r} \left(\frac{1 + R_0/a}{1 + r/a} \right)^2 \quad (42)$$

$\rho_0 = 0.3 \text{ GeV cm}^{-3}$ is the local halo density, $R_0 = 8 \text{ kpc}$ the distance between the Sun and the galactic center, $a = 20 \text{ kpc}$ some length scale. The LKP annihilation rate is then given by

$$\Gamma = \frac{\sigma v}{m^2} \int_0^\infty \rho_{dm}^2 4\pi r^2 dr \quad (43)$$

which leads to a flux of neutrinos at one TeV (assuming a mass of 1 TeV for the LKP) of $4.4 \times 10^{-12} \text{ cm}^{-2} \text{ s}^{-1}$ if the LKP is a KK photon, $2.3 \times 10^{-10} \text{ cm}^{-2} \text{ s}^{-1}$ if the LKP is one flavor of KK neutrino and $2.8 \times 10^{-9} \text{ cm}^{-2} \text{ s}^{-1}$ if the LKP is three flavors of KK neutrino.

Initial state	Final state (zero modes of SM fields)	Feynman diagrams
$B^{(1)} B^{(1)}$	$f \bar{f}$	$t(f_L^{(1)}, f_R^{(1)}), u(f_L^{(1)}, f_R^{(1)})$
$B^{(1)} B^{(1)}$	$\phi \phi^*$	$t(\phi^{(1)}), u(\phi^{(1)}), \text{contact term}$

Table 1: Feynman diagrams for which we calculate the annihilation cross section of a KK photon into SM particles. $s(x)$, $t(x)$ and $u(x)$ denote a tree-level Feynman diagram in which particle x is exchanged in the s -, t - and u -channel respectively. “Contact term” represents the scalar-gauge boson four point interaction. f denotes any zero mode fermion and ϕ is the scalar Higgs doublet.

This is within the sensitivity of some future km^3 neutrino telescopes (like IceCube which will reach a sensitivity of about 10^{-12} in these units at a TeV). If the photon fluxes are of the same order in first approximation, experiments such as MAGIC which will reach about 10^{-12} at a TeV could set constraints on the mass of the LKP. While a large number of experiments are underway, this issue of Kaluza–Klein dark matter detection will be worth pursuing.

Acknowledgements

The authors are grateful for discussions with H.-C Cheng, C.-W. Chiang, B. Dobrescu, J. Jiang and C.E.M. Wagner. We also thank G. Sigl and G. Bertone for enlightening us on the cosmic flux issues. G.S thanks the hospitality of the Service de Physique Théorique du CEA Saclay while part of this work was being completed. This work is supported in part by the US Department of Energy, High Energy Physics Division, under contract W-31-109-Eng-38 and also by the David and Lucile Packard Foundation.

A $B^{(1)}$ Annihilation Cross Sections

In this appendix, we summarize the annihilation cross sections for $B^{(1)}$ into SM fields. In discussing the various processes it is worthwhile to remember some general features of the couplings of the first level KK modes we are considering. First, KK parity insures that only vertices with even numbers of first level KK modes exist. The two important types are couplings of two KK matter fields (fermions or Higgs boson) to a single zero mode gauge boson and coupling of a first level gauge boson to a KK matter field and a zero mode matter field. Recall that the left- and right-handed components of the zero mode fermions each have *separate* massive KK modes, whose couplings to the zero mode gauge bosons are vector-like. When a KK mode gauge boson couples to a KK fermion and a zero-mode fermion, there are generally projectors which insure that the zero mode fermion has the same chirality as the KK fermion.

In the limit in which electroweak symmetry breaking effects are neglected, pairs of $B^{(1)}$ can annihilate into either zero mode fermions, $f\bar{f}$, or pairs of Higgs bosons, $\phi\phi^*$. Figures 4 and 5 show the relevant Feynman diagrams. We approximate all first level KK masses (m) as equal, and ignore all “zero mode” fermion, scalar and gauge boson masses. The cross section for $B^{(1)}B^{(1)} \rightarrow f\bar{f}$ receives contributions in which both the $f_L^{(1)}$ and $f_R^{(1)}$ (in the case of neutrinos only $\nu_L^{(1)}$) are exchanged in both the t - and u - channels. Summing/averaging over final/initial spins and integrating over the phase space of the $f\bar{f}$, the result may be written,

$$\sigma(B^{(1)}B^{(1)} \rightarrow f\bar{f}) = \frac{N_c (g_L^4 + g_R^4) (10 (2m^2 + s) \text{ArcTanh}[\beta] - 7s\beta)}{72 \pi s^2 \beta^2} \quad (44)$$

where β is defined as,

$$\beta = \sqrt{1 - \frac{4m^2}{s}} \quad (45)$$

and for each fermion, $g_L = g_1 Y_L$ and $g_R = g_1 Y_R$. Note that the massless fermions in the final state have prevented interference between the graphs in which $f_L^{(1)}$ is exchanged and $f_R^{(1)}$ is exchanged. The factor N_c sums over the different color combinations allowed in the final state, $N_c = 3$ for quarks and $N_c = 1$ for leptons. Thus, the sum over all three families of SM fermions results in,

$$N_c (g_L^4 + g_R^4) \rightarrow 3g_1^4 (Y_{e_L}^4 + Y_{e_R}^4 + Y_{\nu_L}^4 + 3(Y_{u_L}^4 + Y_{u_R}^4 + Y_{d_L}^4 + Y_{d_R}^4)) = \frac{95}{18} g_1^4. \quad (46)$$

Annihilation into Higgs, with Feynman diagrams shown in Fig. 5, proceeds through t - and u - channel exchange of $\phi^{(1)}$ as well as the four-point interaction of $B^{(1)}B^{(1)}\phi\phi^*$. The cross section is,

$$\sigma(B^{(1)}B^{(1)} \rightarrow \phi\phi^*) = \frac{g_1^4 Y_\phi^4}{6\pi\beta s} \quad (47)$$

where $Y_\phi = 1/2$ and a factor of two is included from the sum over the two complex fields in the scalar doublet. Note that this result implicitly includes the decay (after EWSB effects are properly taken into account) into longitudinal W and Z zero modes as well as the Higgs particle h , as all of these degrees of freedom are included in the scalar doublet. Neglecting EWSB there are no tree-level decays into gauge bosons; such decays are induced by EWSB, but are suppressed by powers of v^2/m^2 and thus we neglect them here.

B $\nu^{(1)}$ Annihilation Cross Sections

The properties of the KK mode of the (left-handed) neutrino are assumed to be approximately independent of the neutrino species. For simplicity, we do not consider the

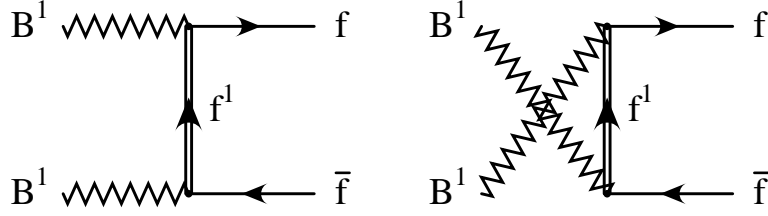


Figure 4: Feynman diagrams for $B^{(1)}B^{(1)}$ annihilation into fermions.

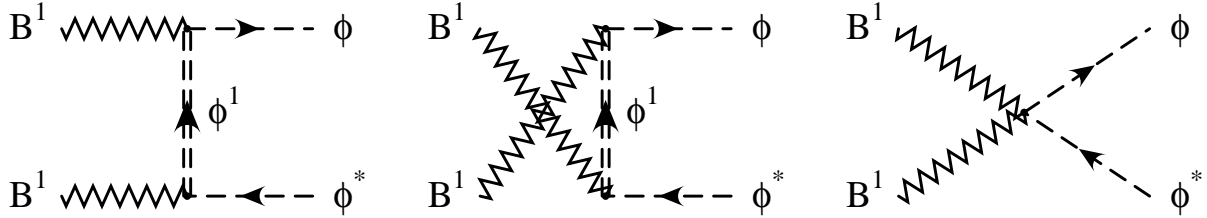


Figure 5: Feynman diagrams for $B^{(1)}B^{(1)}$ annihilation into Higgs scalar bosons.

possibility of a sterile neutrino or its KK modes. For the purposes of this discussion, we assume a neutrino which is the weak partner of the left-handed electron; the results for the weak partners of the muon or tau are simply obtained by appropriately replacing the exchanged particles in specific processes. We continue to neglect fermion and boson masses, and ignore fermion mixing.

The $\nu^{(1)}$ can annihilate with $\bar{\nu}^{(1)}$ into quark (and other family lepton) zero modes through an s -channel Z zero mode (Figure 6). The cross section is given by,

$$\sigma(\nu^{(1)}\bar{\nu}^{(1)} \rightarrow f\bar{f}) = \frac{N_c g_Z^2 (\bar{g}_L^2 + \bar{g}_R^2) (s + 2m^2)}{24\pi\beta s^2}, \quad (48)$$

where,

$$g_Z = \frac{e}{2s_W c_W}, \quad (49)$$

are the couplings of the Z^0 to $\nu^{(1)}\bar{\nu}^{(1)}$ and $\bar{g}_{L(R)}$ are the standard zero mode couplings between the Z^0 and $f\bar{f}$,

$$\bar{g}_{L(R)} = \frac{e}{s_W c_W} [T^3 - Q_f s_W^2] \quad (50)$$

where T^3 is the third component of weak iso-spin of f and Q_f its charge. N_c accounts for the sum over final state color configurations, as before.

Annihilation into zero modes of the charged lepton partner e^+e^- proceeds either through an s -channel Z or a t -channel $W_+^{(1)}$ (Figure 7), or into its own zero modes ($\nu\bar{\nu}$)

Initial state	Final state (zero modes of SM fields)	Feynman diagrams
$\nu^{(1)} \bar{\nu}^{(1)}$	$q \bar{q}$	$s(Z)$
	$\phi \phi^*$	$s(Z)$
	$\nu \bar{\nu}$	$s(Z), t(B^{(1)}, W_3^{(1)})$
	$e^- e^+$	$s(Z), t(W_+^{(1)})$
	$Z^0 Z^0$	$t(\nu^{(1)}, u(\nu^{(1)}))$
$\nu^{(1)} \nu^{(1)}$	$W^- W^+$	$t(e_L^{(1)}), s(Z)$
	$\nu \nu$	$t(B^{(1)}, W_3^{(1)}), u(B^{(1)}, W_3^{(1)})$
$\nu_1^{(1)} \nu_2^{(1)}$	$\nu_1 \nu_2$	$t(Z^{(1)})$

Table 2: Same as Table 1 but for annihilation of the KK neutrino.

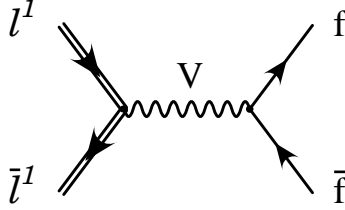


Figure 6: Feynman diagrams for $\nu^{(1)}\bar{\nu}^{(1)}$ annihilation into quarks or leptons of other families.

through an s -channel Z zero mode or by exchanging a t -channel $W_3^{(1)}$ or $B^{(1)}$ (Figure 7). In the limit in which we ignore the mass splitting between $W_3^{(1)}$ and $B^{(1)}$, the exchange of both can be summed into a single $Z^{(1)}$ exchange. The cross section into either zero mode neutrinos of the same flavor or their charged lepton weak partners is,

$$\begin{aligned} \sigma(\nu^{(1)}\bar{\nu}^{(1)} \rightarrow \ell\bar{\ell}) &= \frac{g_Z \hat{g}_L^2 \bar{g}_L [5\beta s + 2(2s + 3m^2)L]}{32 \pi \beta^2 s^2} + \frac{g_Z^2 (\bar{g}_L^2 + \bar{g}_R^2) (s + 2m^2)}{24 \pi \beta s^2} \\ &+ \frac{\hat{g}_L^4 [\beta (4s + 9m^2) + 8m^2 L]}{64 \pi m^2 \beta^2 s} \end{aligned} \quad (51)$$

where $\hat{g}_L = g_Z$,

$$L = \log \left[\frac{1 - \beta}{1 + \beta} \right], \quad (52)$$

and $\bar{g}_{L(R)}$ are given as before. For annihilation into charged leptons, the $\bar{g}_{L(R)}$ should be replaced by the charged lepton values from Eq. 50 and \hat{g}_L now corresponds to the $W_{\pm}^{(1)}$ coupling to $\nu^{(1)}$ and e^0 ,

$$\hat{g}_L^e = \frac{e}{\sqrt{2} s_W}. \quad (53)$$

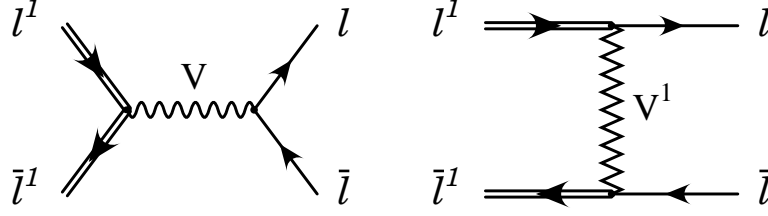


Figure 7: Feynman diagrams for $\nu^{(1)}\bar{\nu}^{(1)}$ annihilation into zero mode leptons of the same family.

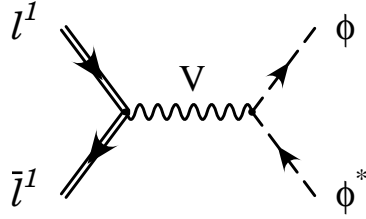


Figure 8: Feynman diagrams for $\nu^{(1)}\bar{\nu}^{(1)}$ annihilation into scalar Higgs bosons.

First modes of $\nu^{(1)}\bar{\nu}^{(1)}$ can annihilate into zero modes of Higgs bosons through an s -channel Z zero mode (Figure 8) with cross section,

$$\sigma(\nu^{(1)}\bar{\nu}^{(1)} \rightarrow \phi_i\phi_i^*) = \frac{g_\phi^2 g_Z^2 (s + 2m^2)}{48\pi\beta s^2}, \quad (54)$$

where the g_Z coupling of $\nu^{(1)}$ to a Z zero mode is as before, and there are two couplings of $\phi\phi^*$ to Z^0 from the charged and neutral entries of the doublet, respectively,

$$g_\phi = \frac{e}{s_W c_W} (T^3 - Q_\phi s_W^2), \quad (55)$$

where the first (upper entry in the doublet) Higgs has charge $Q_\phi = 1$ and the second has $Q = 0$.

Annihilation into ZZ are mediated by t - and u -channel $\nu^{(1)}$, (Figure 9) and has cross section,

$$\sigma(\nu^{(1)}\bar{\nu}^{(1)} \rightarrow ZZ) = \frac{g_Z^4 (2[s^2 + 4m^2s - 8m^4] \text{ArcTanh}[\beta] - \beta s[s + 4m^2])}{8\pi\beta^2 s^3} \quad (56)$$

where g_Z is the coupling to the zero mode Z boson defined above.

Annihilation into W^+W^- zero modes includes t -channel $e_L^{(1)}$ exchange and s -channel annihilation through a virtual Z zero mode (Figure 10). The cross section is,

$$\begin{aligned} \sigma(\nu^{(1)}\bar{\nu}^{(1)} \rightarrow W^+W^-) &= \frac{-5g_{ZW}^2 g_Z^2 [s + 2m^2]}{24\pi\beta s^2} + \frac{g_W^2 g_{ZW} g_Z [\beta s - 2m^2 L]}{8\pi\beta^2 s^2} \\ &\quad - \frac{g_W^4 [\beta(s + 4m^2) + (s + 2m^2)L]}{8\pi\beta^2 s^2} \end{aligned} \quad (57)$$

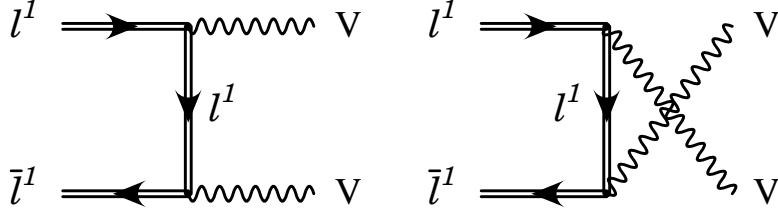


Figure 9: Feynman diagrams for $\nu^{(1)}\bar{\nu}^{(1)}$ annihilation into two neutral vector bosons VV .

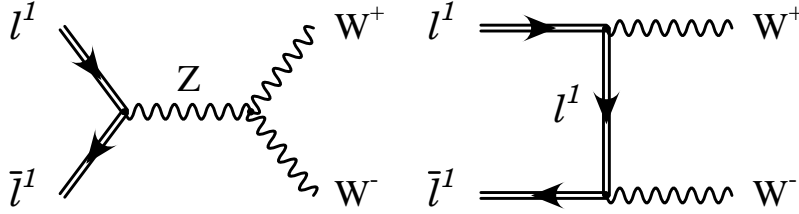


Figure 10: Feynman diagrams for $\nu^{(1)}\bar{\nu}^{(1)}$ annihilation into two charged vector bosons W^+W^- .

where g_Z are the couplings to the Z zero mode as before, g_W is the (vector-like) coupling between the W zero mode to $e_L^{(1)}$ and $\nu^{(1)}$,

$$g_W = \frac{e}{\sqrt{2}s_W}, \quad (58)$$

and g_{ZWW} is the Z - W^+ - W^- coupling between zero modes,

$$g_{ZWW} = e \frac{c_W}{s_W}. \quad (59)$$

Furthermore, $\nu^{(1)}\nu^{(1)}$ ($\bar{\nu}^{(1)}\bar{\nu}^{(1)}$) can annihilate into $\nu\nu$ ($\bar{\nu}\bar{\nu}$) through t - and u -channel exchange of $W_3^{(1)}$ or $B^{(1)}$ (Figure 11). The cross section for annihilation of two neutrinos $\nu^{(1)}\nu^{(1)} \rightarrow \nu\nu$ is given by,

$$\sigma(\nu^{(1)}\nu^{(1)} \rightarrow \nu\nu) = \frac{\hat{g}_L^4(\beta s(2s - m^2) + 2m^2(4s - 5m^2)\text{ArcTanh}[\beta])}{32\pi\beta^2 s^2 m^2} \quad (60)$$

where \hat{g}_L is defined above. Note that if more than one KK neutrino species is present, two related processes will also take two neutrinos of different species into their two zero modes, or one neutrino and one anti-neutrino of different flavors into their zero modes. In both cases, we have a single t -channel Feynman diagram and the cross sections are,

$$\sigma(\nu_1^{(1)}\nu_2^{(1)} \rightarrow \nu_1\nu_2) = \frac{\hat{g}_L^4(4s - 3m^2)}{64\pi\beta sm^2}, \quad (61)$$

$$\sigma(\nu_1^{(1)}\bar{\nu}_2^{(1)} \rightarrow \nu_1\bar{\nu}_2) = \frac{\hat{g}_L^4(\beta(4s + 9m^2) + 8m^2L)}{64\pi\beta^2 sm^2}, \quad (62)$$

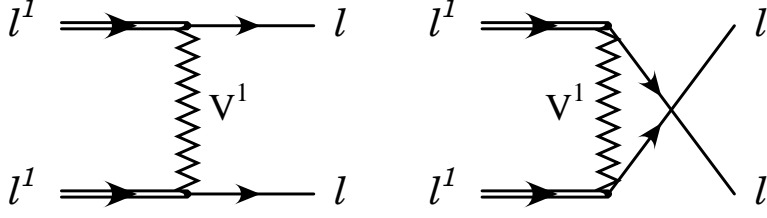


Figure 11: Feynman diagrams for $\nu^{(1)}\nu^{(1)}$ annihilation into two zero mode leptons $\nu\nu$.

Initial state	Final state (zero modes of SM fields)	Feynman diagrams
$e_R^{(1)} \bar{e}_R^{(1)}$	$q \bar{q}$	$s(B^{(0)})$
	$\nu \bar{\nu}$	$s(B^{(0)})$
	$e^- e^+$	$s(B^{(0)}), t(B^{(1)})$
	$\phi \phi^*$	$s(B^{(0)})$
	$Z Z$	$t(e_R^{(1)}), u(e_R^{(1)})$
	$\gamma \gamma$	$t(e_R^{(1)}), u(e_R^{(1)})$
	$Z \gamma$	$t(e_R^{(1)}), u(e_R^{(1)})$
$e_R^{(1)} e_R^{(1)}$	$e^- e^-$	$t(B^{(1)}), u(B^{(1)})$
$e_R^{(1)} B^{(1)}$	$e^- \gamma$	$s(e^-), t(e_R^{(1)})$
	$e^- Z$	$s(e^-), t(e_R^{(1)})$

Table 3: Same as Table 1 but for coannihilation of $e_R^{(1)}$.

with $\hat{g}_L = g_Z$. Finally, we can have cross-flavor transition between $\nu_1^{(1)}\bar{\nu}_2^{(1)}$ into charged lepton zero modes, $e_1^- e_2^+$ through a t -channel $W_{\pm}^{(1)}$ exchange. The corresponding cross section is given by the result for $\sigma(\nu_1^{(1)}\bar{\nu}_2^{(1)} \rightarrow \nu_1\bar{\nu}_2)$ with $\hat{g}_L = e/\sqrt{2}s_W$.

C Coannihilation Cross Sections

The $e_R^{(1)}$ can annihilate with $\bar{e}_R^{(1)}$ into quark (and other family lepton) zero modes through an s -channel $B^{(0)}$ (Figure 6). The cross section is given by,

$$\sigma(e_R^{(1)}\bar{e}_R^{(1)} \rightarrow f\bar{f}) = \frac{N_c g_1^4 Y_{e_R}^2 (Y_{f_L}^2 + Y_{f_R}^2) (s + 2m^2)}{24 \pi \beta s^2}. \quad (63)$$

Note that since $e_R^{(1)}$ is a weak singlet, this formula also applies for annihilation into zero modes of the neutral lepton partner.

Annihilation into e^+e^- zero modes proceeds through an s -channel $B^{(0)}$ or by exchanging a t -channel $B^{(1)}$ (Figure 7). The cross section is,

$$\begin{aligned} \sigma(e_R^{(1)}\bar{e}_R^{(1)} \rightarrow e^+e^-) &= \frac{g_1^4 Y_{e_R}^4 [5\beta s + 2(2s + 3m^2)L]}{32\pi\beta^2 s^2} + \frac{g_1^4 Y_{e_R}^4 [\beta(4s + 9m^2) + 8m^2 L]}{64\pi m^2 \beta^2 s} \\ &+ \frac{g_1^4 Y_{e_R}^2 (Y_{e_R}^2 + Y_{e_L}^2) (s + 2m^2)}{24\pi\beta s^2} \end{aligned} \quad (64)$$

where, L is defined in Section B. Note that we have chosen to include the decay into left-handed electrons in this result, though we could have equally well considered it part of Eq. (63). Evident from comparison of the two equations, this is simply a matter of book-keeping.

Annihilation into zero modes of Higgs bosons occurs through an s -channel $B^{(0)}$ (Figure 8) with cross section,

$$\sigma(e_R^{(1)}\bar{e}_R^{(1)} \rightarrow \phi\phi^*) = \frac{g_1^4 Y_{e_R}^2 Y_\phi^2 (s + 2m^2)}{24\pi\beta s^2}, \quad (65)$$

where the factor of 2 to sum over the two entries of the doublet is included.

Annihilation into ZZ , $Z\gamma$, and $\gamma\gamma$ are mediated by t - and u -channel $e_R^{(1)}$ (Figure 9). This process can be more conveniently described as the single channel $e_R^{(1)}\bar{e}_R^{(1)} \rightarrow B^{(0)}B^{(0)}$, equivalent to the sum of these three γ and Z processes. The cross section is,

$$\sigma(e_R^{(1)}\bar{e}_R^{(1)} \rightarrow B^{(0)}B^{(0)}) = \frac{g_1^4 Y_{e_R}^4 (2[s^2 + 4m^2 s - 8m^4] \text{ArcTanh}[\beta] - \beta s[s + 4m^2])}{8\pi\beta^2 s^3} \quad (66)$$

Annihilation into W^+W^- zero modes is zero in the limit in which one ignores EWSB effects, because $e_R^{(1)}$ is a singlet.

Finally we have the process $e_R^{(1)}e_R^{(1)} \rightarrow e^-e^-$ ($\bar{e}_R^{(1)}\bar{e}_R^{(1)} \rightarrow e^+e^+$) via exchange of a t - or u -channel $B^{(1)}$. This cross section is

$$\sigma(e_R^{(1)}e_R^{(1)} \rightarrow e^-e^-) = \frac{g_1^4 Y_{e_R}^4 (\beta s(2s - m^2) + 2m^2(4s - 5m^2)\text{ArcTanh}[\beta])}{32\pi\beta^2 s^2 m^2}, \quad (67)$$

for lepton KK modes of the same flavor, and,

$$\sigma(e_R^{(1)}\mu_R^{(1)} \rightarrow e^-\mu^-) = \frac{g_1^4 Y_{e_R}^4 (4s - 3m^2)}{64\pi\beta sm^2} \quad (68)$$

$$\sigma(e_R^{(1)}\bar{\mu}_R^{(1)} \rightarrow e^-\mu^+) = \frac{g_1^4 Y_{e_R}^4 (\beta(4s + 9m^2) + 8m^2 L)}{64\pi\beta^2 sm^2} \quad (69)$$

for two modes of different lepton flavor.

Coannihilation of a $B^{(1)}$ with $e_R^{(1)}$ (or $\bar{e}_R^{(1)}$) proceeds into either e^-Z or $e^-\gamma$. In the limit in which the Z mass is disregarded, we can equally well describe this as a single

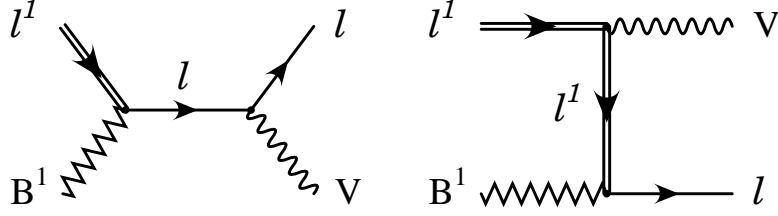


Figure 12: Feynman diagrams for $B^{(1)}f^{(1)}$ annihilation into a zero mode f and vector boson.

channel into $eB^{(0)}$. The cross section is given by,

$$\begin{aligned} \sigma(B^{(1)}e_R^{(1)} \rightarrow B^{(0)}e^-) &= \frac{Y_{e_R}^4 g_1^4 [\beta s(2m^2 - s) + m^2(6m^2 - 2s)L]}{48\pi\beta^2 s^2 m^2} \\ &+ \frac{Y_{e_R}^4 g_1^4 (s - m^2)}{96\pi\beta s m^2} \\ &+ \frac{Y_{e_R}^4 g_1^4 [\beta s(s - 4m^2) - 2m^2(s + 6m^2)L]}{96\pi\beta^2 s^2 m^2} \end{aligned} \quad (70)$$

The KK modes of the left-handed electron are somewhat more complicated because they involve the SU(2) bosons as well as the U(1) boson. We find it convenient to consider neutral zero mode gauge bosons in the $W_3^{(0)}, B^{(0)}$ basis. Annihilation into fermions is given by,

$$\sigma(e_L^{(1)}\bar{e}_L^{(1)} \rightarrow f\bar{f}) = \frac{N_c g^4 (s + 2m^2)}{24\pi\beta s^2}. \quad (71)$$

where the coupling,

$$g^2 = \left(g_1^2 Y_f Y_{e_L} + g_2^2 T_f^3 T_{e_L}^3 \right), \quad (72)$$

is in terms of the hypercharges (Y) and third component of weak iso-spin (T^3) for the fermion and the left-handed electron. For annihilation into zero modes of electrons of the same family we also have t -channel exchange of $B^{(1)}$ and $W_3^{(0)}$, and for annihilation into zero modes of the neutral lepton partner we have t -channel $W_{\pm}^{(1)}$ exchange. Both results may be expressed,

$$\begin{aligned} \sigma(e_L^{(1)}\bar{e}_L^{(1)} \rightarrow e^+e^-, \nu\bar{\nu}) &= \frac{\hat{g}_L^2 g^2 [5\beta s + 2(2s + 3m^2)L]}{32\pi\beta^2 s^2} + \frac{\hat{g}_L^4 [\beta(4s + 9m^2) + 8m^2 L]}{64\pi m^2 \beta^2 s} \\ &+ \frac{g^4 (s + 2m^2)}{24\pi\beta s^2} \end{aligned} \quad (73)$$

where g^2 is defined above, for the specific case of f an electron or neutrino, and $\hat{g}_L = e/2s_W c_W$ for electrons and $\hat{g}_L = e/\sqrt{2}s_W$ for the neutrino final state.

Initial state	Final state (zero modes of SM fields)	Feynman diagrams	
$e_L^{(1)} \bar{e}_L^{(1)}$	$q \bar{q}$	$s(\gamma, Z)$	
	$\nu \bar{\nu}$	$s(Z), t(W_\pm^{(1)})$	
	$e^- e^+$	$s(Z, \gamma), t(B^{(1)}, W_3^{(1)})$	
	$\phi \phi^*$	$s(\gamma, Z)$	
	$Z Z$	$t(e_L^{(1)}), u(e_L^{(1)})$	
	$\gamma \gamma$	$t(e_L^{(1)}), u(e_L^{(1)})$	
	γZ	$t(e_L^{(1)}), u(e_L^{(1)})$	
	$W^+ W^-$	$s(\gamma, Z), u(\nu^{(1)})$	
	$e_L^{(1)} e_L^{(1)}$ $e_L^{(1)} \mu_L^{(1)}$ $\mu_L^{(1)} \bar{e}_L^{(1)}$	$e^- e^-$	$t(B^{(1)}, W_3^{(1)})$
		$e^- \mu^-$	$t(B^{(1)}, W_3^{(1)})$
$\mu^- e^+$		$t(B^{(1)}, W_3^{(1)})$	
$\nu_\mu \bar{\nu}_e$		$t(B^{(1)}, W_\pm^{(1)})$	
$e_L^{(1)} \bar{\nu}^{(1)}$		$q \bar{q}'$	$s(W_-)$
	$e^- \bar{\nu}$	$s(W_-), t(B^{(1)}, W_3^{(1)})$	
	$\phi \phi^*$	$s(W_-)$	
	$Z W^-$	$s(W_-), t(e_L^{(1)}), u(\nu^{(1)})$	
	γW^-	$s(W_-), t(e_L^{(1)}), u(\nu^{(1)})$	
$e_L^{(1)} \nu^{(1)}$ $\mu_L^{(1)} \nu^{(1)}$	$e^- \nu$	$t(B^{(1)}, W_3^{(1)}), u(W_-^{(1)})$	
	$\mu^- \nu$	$t(B^{(1)}, W_3^{(1)})$	
	$\nu_\mu e^-$	$u(W_\pm^{(1)})$	
$\mu_L^{(1)} \bar{\nu}^{(1)}$	$\mu^- \bar{\nu}$	$t(B^{(1)}, W_3^{(1)})$	

Table 4: Same as Table 1 but for coannihilation of $e_L^{(1)}$.

Under our approximation in which EWSB effects are neglected, annihilation of $e_L^{(1)} \bar{e}_L^{(1)}$ into W bosons is equal to the process $\nu^{(1)} \bar{\nu}^{(1)} \rightarrow W^+ W^-$ given in Equation (57), by SU(2) invariance. Similarly, the sum of the annihilation processes into ZZ , γZ , and $\gamma\gamma$ are also equal to the process $\nu^{(1)} \bar{\nu}^{(1)} \rightarrow ZZ$ given in Equation (56) and the sum of annihilation into both components of the Higgs doublet is given by the process $\nu^{(1)} \bar{\nu}^{(1)} \rightarrow \phi\phi^*$ in Equation (54). Furthermore, like-sign annihilation $e_L^{(1)} e_L^{(1)} \rightarrow e^- e^-$ is equal to $\nu^{(1)} \nu^{(1)} \rightarrow \nu\nu$, and thus is given by Equation (60).

$e_L^{(1)} \bar{\nu}^{(1)}$ annihilate into zero modes of quarks or other family leptons through an s -channel $W_-^{(0)}$ with cross section given by Equation (71), replacing with the appropriate charged current coupling: $g^2 \rightarrow g_2^2/2$. Annihilation into leptons of the same family also includes t -channel exchange of $Z^{(1)}$. The cross section is given by Equation (73) with $g^2 \rightarrow g_2^2/2, \hat{g}_L^2 \rightarrow (e/2s_W c_W)^2[-1/2 + s_W^2]$. Annihilation into Higgs occurs through an

s -channel $W_-^{(0)}$ and may be obtained from Equation (54) with the replacement $g_Z^2 g_\phi^2 \rightarrow e^4/4s_W^4$. Annihilation into gauge bosons is most simply described in terms of annihilation into $W^- B^{(0)}$, and $W^- W_3^{(0)}$. The first process is mediated by t -channel $e_L^{(1)}$ exchange and u -channel $\nu^{(1)}$ exchange, and is given by Equation (56) with $g_Z^2 \rightarrow -e^2/2\sqrt{2}s_W c_W$. The second is simply obtained from $\nu^{(1)}\bar{\nu}^{(1)} \rightarrow W^+ W^-$ in Equation (57) by SU(2) invariance. Finally, $e_L^{(1)}\nu^{(1)} \rightarrow e^- \nu$ is mediated by t -channel $Z^{(1)}$ and u -channel $W_\pm^{(1)}$ exchange, and is given by,

$$\begin{aligned} \sigma(e_L^{(1)}\nu^{(1)} \rightarrow e^- \nu) &= \frac{g_t^2 g_u^2 [4m^2(4s - 5m^2)\text{ArcTanh}[\beta] + m^2\beta s]}{32\pi\beta^2 s^2 m^2} \\ &+ \frac{\beta s [(g_t^4 + g_u^4)(4s - 3m^2)]}{64\pi\beta^2 s^2 m^2}, \end{aligned} \quad (74)$$

with $g_t^2 = e^2/(2s_W^2 c_W^2)(-1/2 + s_W^2)$ and $g_u^2 = e^2/2s_W^2$

If there are multiple families of KK left-handed electrons or neutrinos, there will also be flavor-changing annihilation of $\mu_L^{(1)}\nu^{(1)} \rightarrow \mu^- \nu$, $\mu_L^{(1)}\nu^{(1)} \rightarrow \nu_\mu e^-$, and $\mu_L^{(1)}\bar{\nu}^{(1)} \rightarrow \mu^- \bar{\nu}$. The cross sections for the first two processes are both given by Equation (61), with the replacements $\hat{g}_L^2 \rightarrow e^2/(2s_W^2 c_W^2)(-1/2 + s_W^2)$, and $\hat{g}_L^2 \rightarrow e^2/2s_W^2$. The cross section for $\mu_L^{(1)}\bar{\nu}^{(1)} \rightarrow \mu^- \bar{\nu}$ is given by Equation (62) with the replacement $\hat{g}_L^2 \rightarrow e^2/(2s_W^2 c_W^2)(-1/2 + s_W^2)$.

References

- [1] J. R. Primack, *Cosmological parameters*; astro-ph/0007187.
- [2] M. S. Turner, *A New Era in Determining the Matter Density*; astro-ph/0106035.
- [3] E. W. Kolb and R. Slansky, Phys. Lett. B **135**, 378 (1984).
- [4] K. R. Dienes, E. Dudas and T. Gherghetta, Nucl. Phys. B **537**, 47 (1999) [arXiv:hep-ph/9806292].
- [5] T. Appelquist, H. C. Cheng and B. A. Dobrescu, Phys. Rev. D **64**, 035002 (2001) [arXiv:hep-ph/0012100].
- [6] N. Arkani-Hamed, S. Dimopoulos and G. R. Dvali, Phys. Lett. B **429**, 263 (1998) [arXiv:hep-ph/9803315]; L. Randall and R. Sundrum, Phys. Rev. Lett. **83**, 3370 (1999) [arXiv:hep-ph/9905221].
- [7] I. Antoniadis, C. Munoz and M. Quiros, Nucl. Phys. B **397**, 515 (1993) [arXiv:hep-ph/9211309]. I. Antoniadis, K. Benakli and M. Quiros, Phys. Lett. B **331**, 313 (1994) [arXiv:hep-ph/9403290]. I. Antoniadis, S. Dimopoulos, A. Pomarol and M. Quiros, Nucl. Phys. B **544**, 503 (1999) [arXiv:hep-ph/9810410].

- [8] B. A. Dobrescu and E. Poppitz, Phys. Rev. Lett. **87**, 031801 (2001) [arXiv:hep-ph/0102010].
- [9] T. Appelquist, B. A. Dobrescu, E. Ponton and H. U. Yee, Phys. Rev. Lett. **87**, 181802 (2001) [arXiv:hep-ph/0107056].
- [10] H. C. Cheng, B. A. Dobrescu and C. T. Hill, Nucl. Phys. B **589**, 249 (2000) [arXiv:hep-ph/9912343].
- [11] N. Arkani-Hamed, H. C. Cheng, B. A. Dobrescu and L. J. Hall, Phys. Rev. D **62**, 096006 (2000) [arXiv:hep-ph/0006238].
- [12] H. J. He, C. T. Hill and T. M.P. Tait, Phys. Rev. D **65**, 055006 (2002) [arXiv:hep-ph/0108041].
- [13] R. Barbieri, L. J. Hall and Y. Nomura, Phys. Rev. D **63**, 105007 (2001) [arXiv:hep-ph/0011311].
- [14] N. Arkani-Hamed and M. Schmaltz, Phys. Rev. D **61**, 033005 (2000) [arXiv:hep-ph/9903417].
- [15] R. N. Mohapatra and A. Perez-Lorenzana, arXiv:hep-ph/0205347.
- [16] E. A. Mirabelli and M. Schmaltz, Phys. Rev. D **61**, 113011 (2000) [arXiv:hep-ph/9912265].
- [17] G. R. Dvali and M. A. Shifman, Phys. Lett. B **475**, 295 (2000) [arXiv:hep-ph/0001072].
- [18] D. E. Kaplan and T. M.P. Tait, JHEP **0006**, 020 (2000) [arXiv:hep-ph/0004200]; D. E. Kaplan and T. M.P. Tait, JHEP **0111**, 051 (2001) [arXiv:hep-ph/0110126].
- [19] T. Appelquist, B. A. Dobrescu, E. Ponton and H. U. Yee, arXiv:hep-ph/0201131.
- [20] G. von Gersdorff, N. Irges and M. Quiros, arXiv:hep-th/0204223.
- [21] H. C. Cheng, K. T. Matchev and M. Schmaltz, arXiv:hep-ph/0204342.
- [22] H. Georgi, A. K. Grant and G. Hailu, Phys. Lett. B **506**, 207 (2001) [arXiv:hep-ph/0012379].
- [23] T. G. Rizzo, Phys. Rev. D **64**, 095010 (2001) [arXiv:hep-ph/0106336]; C. Macesanu, C. D. McMullen and S. Nandi, arXiv:hep-ph/0201300; H. C. Cheng, K. T. Matchev and M. Schmaltz, arXiv:hep-ph/0205314.
- [24] N. Arkani-Hamed, A. G. Cohen and H. Georgi, Phys. Rev. Lett. **86**, 4757 (2001) [arXiv:hep-th/0104005]; C. T. Hill, S. Pokorski and J. Wang, Phys. Rev. D **64**, 105005 (2001) [arXiv:hep-th/0104035].

- [25] E. W. Kolb and M. S. Turner, *Redwood City, USA: Addison-Wesley (1990) 547 p. (Frontiers in physics, 69).*
- [26] K. Griest and D. Seckel, *Three Exceptions In The Calculation Of Relic Abundances;* Phys. Rev. D **43**, 3191 (1991).
- [27] M. E. Peskin and T. Takeuchi, Phys. Rev. D **46**, 381 (1992).
- [28] See, for example, M. E. Peskin and J. D. Wells, Phys. Rev. D **64**, 093003 (2001) [arXiv:hep-ph/0101342]; D. Choudhury, T. M.P. Tait and C. E. Wagner, arXiv:hep-ph/0202162.